Ultrasonics Sonochemistry 92 (2023) 106269

Contents lists available at ScienceDirect

Ultrasonics Sonochemistry

journal homepage: www.elsevier.com/locate/ultson

Synergistic bactericidal effect of ultrasound combined with citral nanoemulsion on *Salmonella* and its application in the preservation of purple kale

Hui Yang [a], Luyi Song [a], Peiwen Sun [a], Ruiying Su [a], Shuqi Wang [a], Shuai Cheng [a], Xiangjun Zhan [a], Xin Lü [a], Xiaodong Xia [b], Chao Shi [a,*]

[a] College of Food Science and Engineering, Northwest A&F University, Yangling, Shaanxi 712100, China
[b] School of Food Science and Technology, National Engineering Research Center of Seafood, Dalian Polytechnic University, Dalian, Liaoning 116304, China

ARTICLE INFO

Keywords:
Ultrasound
Citral nanoemulsion
Salmonella Typhimurium
Purple kale
Synergistic antibacterial effect
Germicidal mechanism

ABSTRACT

In this study, a novel citral nanoemulsion (CLNE) was prepared by ultrasonic emulsification. The synergistic antibacterial mechanism of ultrasound combined with CLNE against *Salmonella* Typhimurium and the effect on the physicochemical properties of purple kale were investigated. The results showed that the combined treatment showed obviously inactivate effect of *S*. Typhimurium. Treatment with 0.3 mg/mL CLNE combined with US (20 kHz, 253 W/cm^2) for 8 min reduced *S*. Typhimurium populations in phosphate-buffered saline (PBS) by 9.05 log CFU/mL. Confocal laser scanning microscopy (CLSM), flow cytometry (FCM), protein and nucleic acid release assays showed that the US combination CLNE disrupt the integrity of *S*. Typhimurium membranes. Reactive oxygen species (ROS) and malondialdehyde (MDA) detection indicated that US+CLNE exacerbated oxidative stress and lipid peroxidation in cell membranes. The morphological changes of cells after different treatments by field emission scanning electron microscopy (FESEM), transmission electron microscopy (TEM) illustrated that the synergistic effect of US+CLNE treatment changed the morphology and internal microstructure of the bacteriophage cells. Application of US+CLNE on purple kale leaves for 6 min significantly ($P < 0.05$) reduced the number of *S*. Typhimurium, but no changes in the physicochemical properties of the leaves were detected. This study elucidates the synergistic antibacterial mechanism of ultrasound combined with CLNE and provides a theoretical basis for its application in food sterilization.

1. Introduction

Food safety is a global public health concern that affects hundreds of millions of people who become ill from eating food contaminated with foodborne pathogenic bacteria, and costs significant resources to do so. *Salmonella* is one of the main bacteria that threaten food safety and is responsible for a multitude of foodborne illnesses worldwide [1]. The European Centre for Disease Prevention and Control (ECDC) reported that *Salmonella* accounted for 33% of the 5,146 foodborne illnesses reported in European Union (EU) member states in 2018 [2]. Meanwhile, *Salmonella* can cause contamination of tomatoes, bean sprouts and other fruits and vegetables [3]. Purple kale, which is often eaten raw as a vegetable with anti-aging and weight loss properties, can be considered a food with a high risk of spreading *Salmonella* [4].

Synthetic bacteriostatic agents are widely used in the food industry to inactivate microorganisms [5]. Sodium hypochlorite is the most commonly used disinfectant to kill pathogenic bacteria on food surfaces [6]. However, the presence of organic matter limits the bactericidal activity of sodium hypochlorite [7]. Essential oils (EOs) extracted from different parts of aromatic plants are safe, efficient and non-toxic, and these bioactive compounds have a wide range of antibacterial and antiseptic properties [8]. Their antibacterial efficacy is related to their chemical composition, with phenolic and aldehyde components being the main compounds that cause bacterial inactivation [9]. However, the hydrophobic, highly volatile and unstable physical properties of essential oils limit their wide application [10].

Nanoemulsions are non-thermodynamically stable colloidal dispersion systems. By virtue of the dispersed phase, they can be classified as water-in-oil (W/O), oil-in-water (O/W) or bicontinuous [11]. The droplet size of nanoemulsions ranges from 20 to 200 nm, and the narrow

* Corresponding author at: College of Food Science and Engineering, Northwest A&F University, 22 Xinong Road, Yangling, Shaanxi 712100, China.
E-mail address: meilixinong@nwsuaf.edu.cn (C. Shi).

https://doi.org/10.1016/j.ultsonch.2022.106269
Received 24 November 2022; Received in revised form 8 December 2022; Accepted 12 December 2022
Available online 21 December 2022

size distribution increases the surface area [12]. Due to the increased contact surface, the resulting small droplets enhance the bioactivity and kinetic stability of the dispersed medium [13]. Thus, nanoemulsions are a very effective delivery system for loading, encapsulation and enhancing bioavailability of bioactive compounds, among others [14].

Ultrasound is commonly used in the food industry as an important non-thermal physical sterilization process. The cavitation effect of ultrasound is the most influential factor in its bactericidal ability [15]. Ultrasonic waves generate bubbles in the liquid medium with violent vibrations. At the moment of bubble rupture, local high temperatures are generated. In addition, strong liquid shear and shock waves can affect the wall/membrane structure [16,17]. However, the antimicrobial effect of ultrasound alone is limited without damaging the quality of the product, so combining ultrasound with other sterilization technologies may be an effective bactericidal approach [18]. To our knowledge, there are few studies on the combination of ultrasound (US) and citral nanoemulsions (CLNE), and their joint action against *Salmonella* has not been reported.

In the present work, we investigated the antibacterial effect of US+CLNE against *Salmonella* and the possible underlying mechanisms. On this basis, the effect of US+CLNE on the physicochemical properties of purple kale was investigated.

2. Materials and methods

2.1. Bacterial inoculum preparation

Salmonella enterica subsp. *enterica* serovar Typhimurium ATCC 14028 was derived from the American Type Culture Collection (ATCC; Manassas, VA, USA). Bacteria were incubated in LB broth at 37 °C with shaking at 130 rpm for 12 h. Bacteria were collected by centrifugation at 8000 × *g* for 5 min at 4 °C, washed twice with sterile phosphate-buffered saline (PBS, pH 7.2), and finally resuspended for use. The initial concentration of bacteria was 10^9 CFU/mL.

2.2. Preparation of nanoemulsions

Citral (CAS: 5392-40-5) was from Chengdu Must Bio-technology Co., Ltd. (Chengdu, Sichuan, China) with a purity of ≥ 99.2% by HPLC. Tween 80 (CAS: 9005-65-6) was purchased from Shanghai Yuanye Biotechnology Co., Ltd. (Shanghai, China).

CLNE was carried out using the approach of Prakash et al [19] with partial modifications. Specifically, citral was mixed 1:2 with Tween 80 and stirred for 10 min at room temperature at 1100 rpm, then water was added to 10 mL and continued to stir for 30 min to prepare the crude emulsion. The nanoemulsions were treated with an ultrasonic crusher (Scientz-II D; Ningbo Scientz, Zhejiang, China) at 70% power for 9 min with a pulse time of 5 s on / 5 s off to reduce the size distribution of the nanoemulsions.

2.3. Characterization of EO emulsions

The mean droplet size (Z-average), polydispersity index (PDI) and ζ-potential of CLNE were evaluated by dynamic light scattering using the Nano ZEN3600 Malvern Zetasizer (Malvern Instruments Limited, Worcestershire, UK). Prior to the measurements, the samples were diluted 1:100 with distilled water to eliminate multiple scattering effects. All measurements were repeated at 25 °C.

2.4. Antibacterial treatments

The bacterial suspensions were treated with ultrasound, CLNE, and US+CLNE, respectively. For the ultrasound treatment, the method of Guo et al [20] as followed with some modifications. Ultrasound treatment was performed with a 6-mm diameter ultrasonic probe (Scientz-II D, Ningbo Scientz, Zhejiang, China). The device was equipped with a temperature chamber (DC-1006, Safety, Ningbo, China) to prevent drastic temperature fluctuations during treatment. Samples were injected into sterile cylindrical glass vials with the probe immersed at least 2 cm below the liquid surface. Ultrasound parameters were 115, 184 and 253 W/cm^2 and treatment times were 2, 4, 6 and 8 min with a pulse time of 2 s on / 2 s off.

CLNE concentrations of 0.2 and 0.3 mg/mL were predetermined based on the minimum inhibitory concentration (MIC) performed in our laboratory (data not shown). CLNE was added to sample at citral concentrations and cell densities of 0.2, 0.3 mg/mL and 10^9 CFU/mL, respectively. The sample was incubated at room temperature for 2, 4, 6 and 8 min.

In the combined treatment, samples with CLNE added was sonicated. After each treatment, samples were serially diluted and coated on LB agar, incubated at 37 °C for 18 h. Inactivation of *S*. Typhimurium was assessed by calculating the log reduction of the treated samples compared to the control group.

2.5. Field emission scanning electron microscopy (FESEM) observation

FESEM followed the method of He et al [21] with slight modifications. The treated samples were collected (5000 × *g*, 4 °C, 10 min) and fixed overnight at 4 °C with 2.5% (v/v) glutaraldehyde. The samples were dehydrated with graded ethanol (30, 50, 70, 80, 90, 100%), and the bacterial solution was added dropwise on a φ6 slide and then fixed on a FESEM holder. Finally, samples were sprayed with gold under vacuum and observed with FESEM (S-4800; Hitachi, Tokyo, Japan).

2.6. Transmission electron microscopy (TEM) observation

TEM was performed by referring to the method of Liao et al [22] with slight modifications. Briefly, samples were collected and fixed with 2.5% (v/v) glutaraldehyde aqueous solution at 4 °C for 5 h. Cryo-agar embedding at 35 °C was followed by continued fixation for 12 h. Samples were embedded in capsules containing white glue and then sectioned at 70–90 nm on a copper grid and stained with lead citrate and uranyl acetate. Finally, these samples were observed on TEM (H-7650; Hitachi, Japan).

2.7. Determination of protein and nucleic acids release

The method reported by Zhang et al [23], with appropriate modifications, was used to analyze the release of proteins and nucleic acids from bacterial. Specifically, supernatants of *S*. Typhimurium treated with different treatments were collected. The absorbance of the supernatants at 260 nm and 280 nm was measured with an ultraviolet-visible spectrophotometer (UV-2550, Shimadzu, Tokyo, Japan) to quantify the amount of nucleic acid and soluble protein released from *S*. Typhimurium.

2.8. Measurement of reactive oxygen species (ROS) levels

ROS levels of *S*. Typhimurium were based on the method of Díaz-García et al [24] with slight modifications. *S*. Typhimurium was diluted to 10^7 CFU/mL. Treated samples were collected and a DCFH-DA fluorescent probe (final concentration 5 μM) was added. After incubation at 37 °C for 10 min protected from light, the probe was washed and then the fluorescence intensity was detected in real time using a multi-mode zymography (SpectraMax M2, Molecular Devices, San Jose, CA, USA). The excitation and emission wavelengths were 488 nm and 525 nm, respectively. ROS data were normalized by the amount of viable bacteria in the cell suspension.

2.9. Measuring of extracellular malondialdehyde

Extracellular MDA was determined as described by Cao et al [25]

with slight modifications. The absorbance values of supernatants at 450 nm, 532 nm and 600 nm were determined using a multi-mode zymography (Spectra Max M2) according to the instructions of the lipid peroxidation MDA assay kit (Solarbio Life Sciences, Beijing, China). MDA content (nmol/mL) = $5 \times (12.9 \times (\Delta A_{532\ nm} - \Delta A_{600\ nm}) - 2.58 \times \Delta A_{450\ nm})$.

2.10. Confocal laser scanning microscopy (CLSM) analysis

The method of Tian et al [26] was used with some modifications. Samples were collected and washed twice with 0.85% (v/v) NaCl. Add 2 × staining solution (SYTO 9/PI) to the bacterial suspension and incubate for 15 min in the dark. Subsequently, 5-μL bacterial suspensions were transferred to slides and observed under a CLSM (A1, Nikon, Tokyo, Japan).

2.11. Measuring membrane integrity of S. Typhimurium by flow cytometry

Flow cytometry was performed according to the method of Nieto-Velázquez et al [27], with slight modifications. For live cells, samples were collected (8000× *g*, 4 °C, 2 min) and resuspended with 0.85% (v/v) NaCl. Dead cell suspensions were prepared by mixing bacteria killed by 75% (v/v) isopropanol in equal proportions with the live bacterial solution. The treated samples were collected and the bacterial amounts were all diluted to 1×10^8 CFU/mL. Samples mixed by SYTO 9 or PI were incubated for 15 min at room temperature in the dark and read by flow cytometry (CytoFLEX; Beckman, Shanghai, China).

2.12. Application of combined treatment on purple kale

2.12.1. Preparation of purple kale

Purple kale was obtained from a local market (Yangling, China), stored at 4 °C, and consumed within 2 days. The preparation was performed according to the method of Kang et al [28] with slight modifications. Briefly, purple kale was rinsed with tap water to remove surface impurities. Afterwards, purple kale was cut into 3 × 3 cm, approximately 0.5 cm (1.9 ± 0.21 g) thick leaves by a sterile knife. Prior to inoculation, leaves were soaked in 75% (v/v) alcohol for 5 min and then UV-C irradiated for 15 min. The PBS from the homogenized leaves was applied to LB medium and no possible residual background microorganisms were found.

The 100 μL suspension of *S*. Typhimurium was spot inoculated onto the surface of purple kale. The leaves were dried for at least 1.5 h to allow the pathogen to thoroughly adhere to the surface of purple kale.

2.12.2. Washing and processing of purple kale

The washing method was based on that reported by Duarte et al [4] with appropriate modifications. The experimental treatments included ultrapure water (UW), US (253 W/cm^2), CLNE (0.2, 0.3 mg/mL) and US+CLNE, all with a treatment time of 6 min. Samples without any treatment after inoculation were used as controls.

2.12.3. Microbiological analysis

Immediately after treatment with 2.12.2, two grams of purple kale leaves were homogenized in a sterile homogenization bag containing 10 mL of PBS for 2 min. The homogenate was serially diluted with PBS and applied in LB plates for 18 h at 37 °C.

2.13. Quality assessment of purple kale

To underscore the impact of different treatments on the characteristics of purple kale, pH, color and hardness of the leaves were evaluated at days 0, 3 and 7 of storage.

Table 1
Average droplet size (Z-average), polydispersity index (PDI) and zeta-potential of CLNE.

CLNE	Z-average (nm)	PDI	ζ-potential (mV)
	29.4 ± 0.1	0.291 ± 0.006	-18.93 ± 1.39

2.13.1. Determination of pH

The homogenization process of purple kale leaves was performed according to 2.12.3. The pH was measured at room temperature (25 °C) using a pH meter (Mettler-Toled S.p.A., MI, Italy).

2.13.2. Color analysis

Color changes in purple kale were measured with a ColorFlex® EZ colorimeter (CS-820, Color Spectrum Technology Ltd., Hangzhou, China). For the different treatments, five readings were taken from different positions of the purple kale.

The total color difference was calculated using Equation (1) Fan et al [29].

$$\sqrt{(L^* - L_0^*)^2 + (a^* - a_0^*)^2 + (b^* - b_0^*)^2} \quad (1)$$

where L_0^*, a_0^* and b_0^* were the color values of the standard samples in the control group.

2.13.3. Hardness measurement

Hardness measurements of kale leaves were carried out with a texture analyzer (TA. XT PLUS/50, Stable Micro System Ltd., Godalming, UK). The pre-test, test and post-test speeds were set at 1.00, 1.00 and 10.00 mm/s, respectively. Texture Expert software (Stable Micro System Ltd.) used the peak force as hardness (kg). The results of each treatment were performed in five copies.

2.14. Statistical analyses

Experimental data were expressed as mean ± standard deviation (SD) with three replications (n = 3). Statistical differences were assessed using SPSS version 20.0 (SPSS 20.0, SPSS Inc., Chicago, IL, USA). One-way analysis of variance (ANOVA) and Duncan's multiple test were used to test for statistical significance. Differences of $P < 0.05$ were considered statistically significant, and different letters indicate significant differences.

3. Results

3.1. Characterization of nanoemulsion

As shown in Table 1, the freshly prepared citral nanoemulsions (CLNE) had a Z-average of 29.4 ± 0.1 nm and a PDI of 0.291 ± 0.006, demonstrating the good particle size distribution of the nanoemulsions in this study. The ζ-potential of -18.93 ± 1.39 mV indicates the low stability possessed by this nanoemulsion.

3.2. Antibacterial effect of different treatments against S. Typhimurium

The inactivation of *S*. Typhimurium by single or combined treatments of US and CLNE is shown in Table 2. For US individual treatment, *S*. Typhimurium populations were reduced by 0.41–1.81 log CFU/mL within 2–8 min. Inactivation of *S*. Typhimurium by ultrasound of the same power showed a time dependence. *S*. Typhimurium populations decreased by 0.23–0.57 log CFU/mL after 2–8 min of CLNE treatment at 0.2 and 0.3 mg/mL. In contrast to the separate treatments of US and CLNE, US+CLNE showed a significant ($P < 0.05$) increase in the reduction of *S*. Typhimurium. Specifically, US+0.2 mg/mL CLNE treatment for 2–4 min did not achieve the cumulative effect of both

Table 2
Reduction of *S*. Typhimurium populations after treatment with US, CLNE and US+CLNE, respectively.

Time /min	US (reduction log CFU/mL)			CLNE (reduction log CFU/mL)		CLNE+US (reduction log CFU/mL)					
						US+0.2 mg/mL CLNE			US+0.3 mg/mL CLNE		
	115 W/cm^2	184 W/cm^2	253 W/cm^2	0.2 mg/mL CLNE	0.3 mg/mL CLNE	115 W/cm^2	184 W/cm^2	253 W/cm^2	115 W/cm^2	184 W/cm^2	253 W/cm^2
2	0.41 ± 0.06^{Ab}	0.45 ± 0.08^{Ab}	0.48 ± 0.07^{Ab}	0.23 ± 0.08^{Aa}	0.33 ± 0.19^{Aab}	0.64 ± 0.13^{Ac}	0.76 ± 0.08^{Ac}	0.91 ± 0.14^{Ad}	1.48 ± 0.08^{Ae}	1.69 ± 0.18^{Af}	2.82 ± 0.16^{Ag}
4	0.50 ± 0.11^{Ab}	0.70 ± 0.12^{Bc}	0.83 ± 0.15^{Bcd}	0.32 ± 0.06^{Ba}	0.37 ± 0.12^{Aab}	0.83 ± 0.15^{Bcd}	0.93 ± 0.12^{Bd}	1.19 ± 0.16^{Be}	3.46 ± 0.18^{Bf}	3.62 ± 0.10^{Bg}	4.23 ± 0.11^{Bh}
6	0.80 ± 0.16^{Bab}	1.16 ± 0.12^{Cb}	1.24 ± 0.19^{Cbc}	0.38 ± 0.03^{BCa}	0.42 ± 0.05^{ABa}	1.93 ± 0.17^{Ccd}	2.01 ± 0.09^{Cd}	2.96 ± 0.13^{Ce}	4.12 ± 0.14^{Cf}	4.25 ± 0.12^{Bf}	6.27 ± 0.14^{Cg}
8	1.11 ± 0.19^{Cb}	1.44 ± 0.16^{Dc}	1.81 ± 0.19^{Dd}	0.43 ± 0.08^{Ca}	0.57 ± 0.11^{Ba}	3.57 ± 0.15^{De}	4.45 ± 0.17^{Df}	5.31 ± 0.16^{Dg}	4.50 ± 0.08^{Df}	6.22 ± 0.17^{Ch}	9.07 ± 0^{Di}

Results are expressed as mean ± SD. Different upper- and lower-case letters indicate statistically significant differences ($P < 0.05$) for any mean in the same column or row.

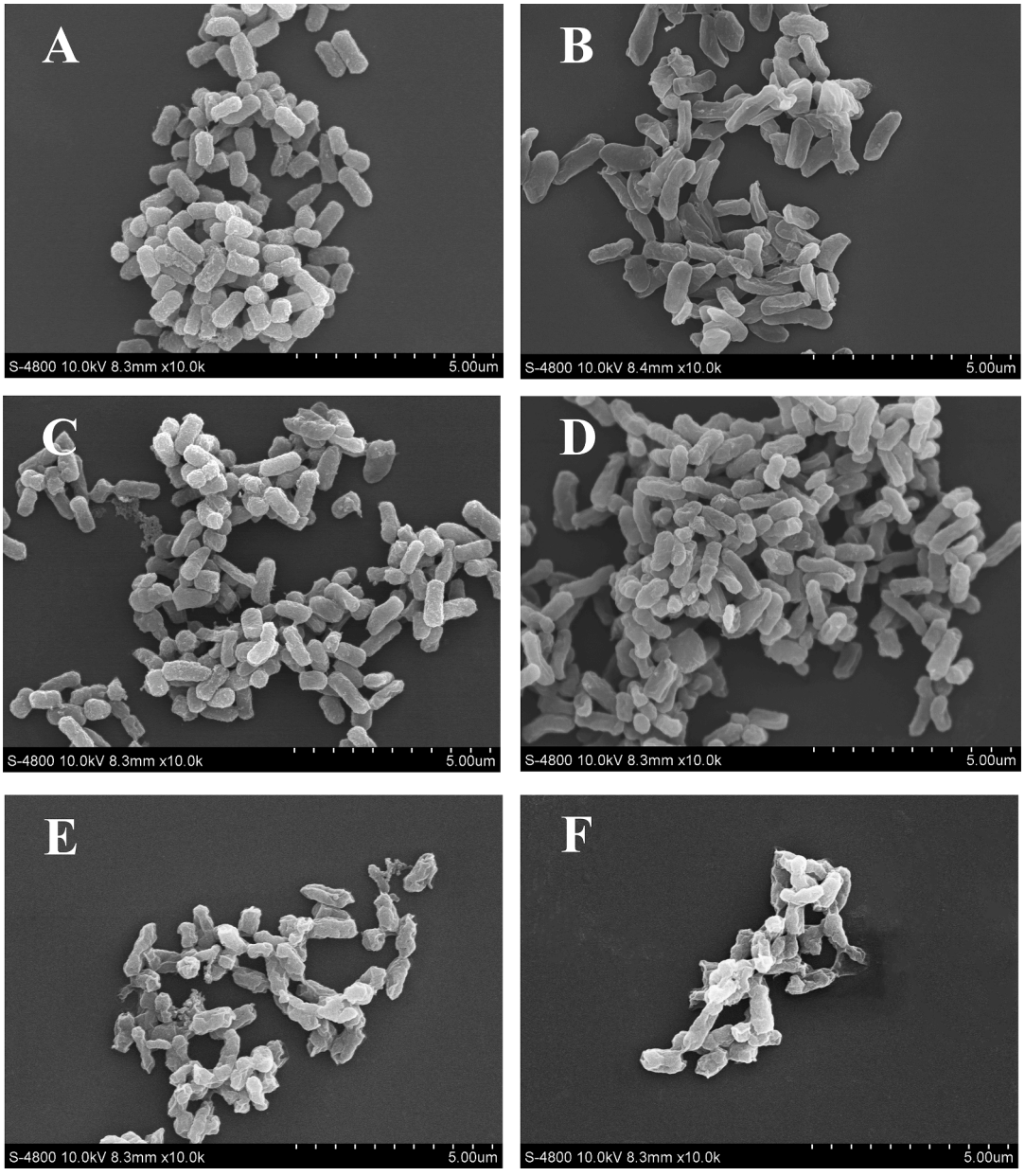

Fig. 1. FESEM images of *S*. Typhimurium after different treatments. A, Control (untreated); B, US (253 W/cm^2); C, 0.2 mg/mL CLNE; D, 0.3 mg/mL CLNE; E, US+0.2 mg/mL CLNE; F, US+0.3 mg/mL CLNE. The duration of action was 6 min for all treatment groups. Magnification = 10,000 ×, bar marker = 5.00 μm.

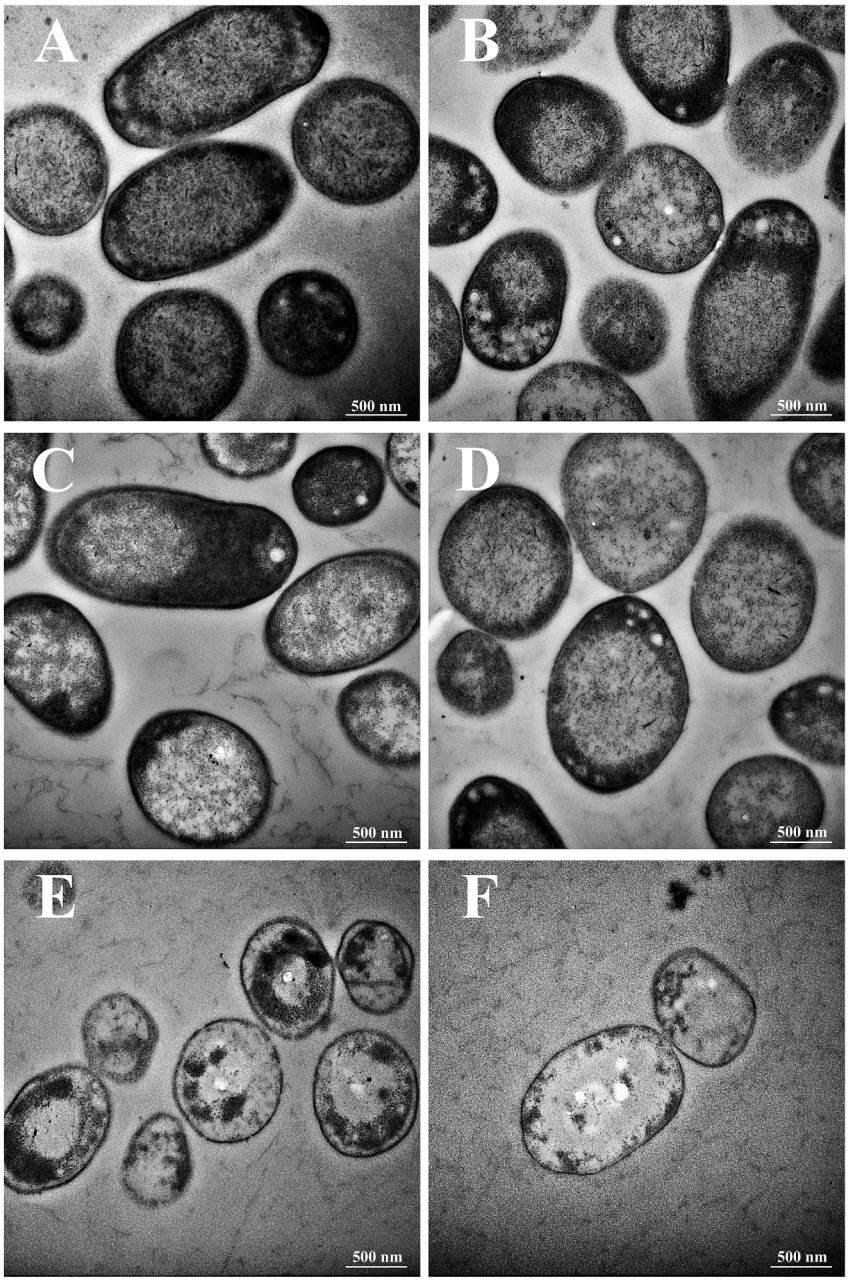

Fig. 2. TEM images of *S*. Typhimurium after different treatments. A, Control (untreated); B, US (253 W/cm^2); C, 0.2 mg/mL CLNE; D, 0.3 mg/mL CLNE; E, US+0.2 mg/mL CLNE; F, US+0.3 mg/mL CLNE. The duration of action was 6 min for all treatment groups. Magnification = 30,000 ×, bar marker = 500 nm.

treatments alone. When the treatment time was extended to 6 and 8 min, there was a clear synergistic effect of US+0.2 mg/mL CLNE on the inactivation of *S*. Typhimurium. For US+0.3 mg/mL CLNE, *S*. Typhimurium was subjected to a distinctly higher synergistic effect than US+0.2 mg/mL CLNE. In particular, US (253 W/cm^2)+0.3 mg/mL CLNE reduced *S*. Typhimurium by 9.07 log CFU/mL and the bacterial load reached the limit value.

3.3. Changes to the surface morphology of S. Typhimurium

In the control group, cells of *S*. Typhimurium showed typical rod or bar morphology with smooth, intact and full surfaces and tight junctions between the organisms (Fig. 1A). After ultrasound treatment alone, the vast majority of cells still had relatively intact rod-like structures, but the morphology was dried and flattened, and individuals were more dispersed from one another (Fig. 1B). CLNE treatments at 0.2 and 0.3 mg/mL were not obviously distinguished from the control group, and the difference in cell morphology caused by 0.3 mg/mL CLNE was higher than that of 0.2 mg/mL (Fig. 1C, D). US+0.2 mg/mL CLNE had more prominent morphological changes with cell membrane wrinkling, adhesions between cells, and looser cell distribution compared to US or CLNE alone (Fig. 1E). *S*. Typhimurium undergoing US+0.3 mg/mL CLNE treatment showed the greatest degree of collapse, with cells completely dried out and crumpled, most cells completely adherent, and some cell walls and membranes completely damaged (Fig. 1F).

3.4. Changes in the internal ultrastructure of S. Typhimurium

Fig. 2A shows the typical rod-like structure of *S*. Typhimurium with a smooth, continuous and intact cell wall/membrane and uniform

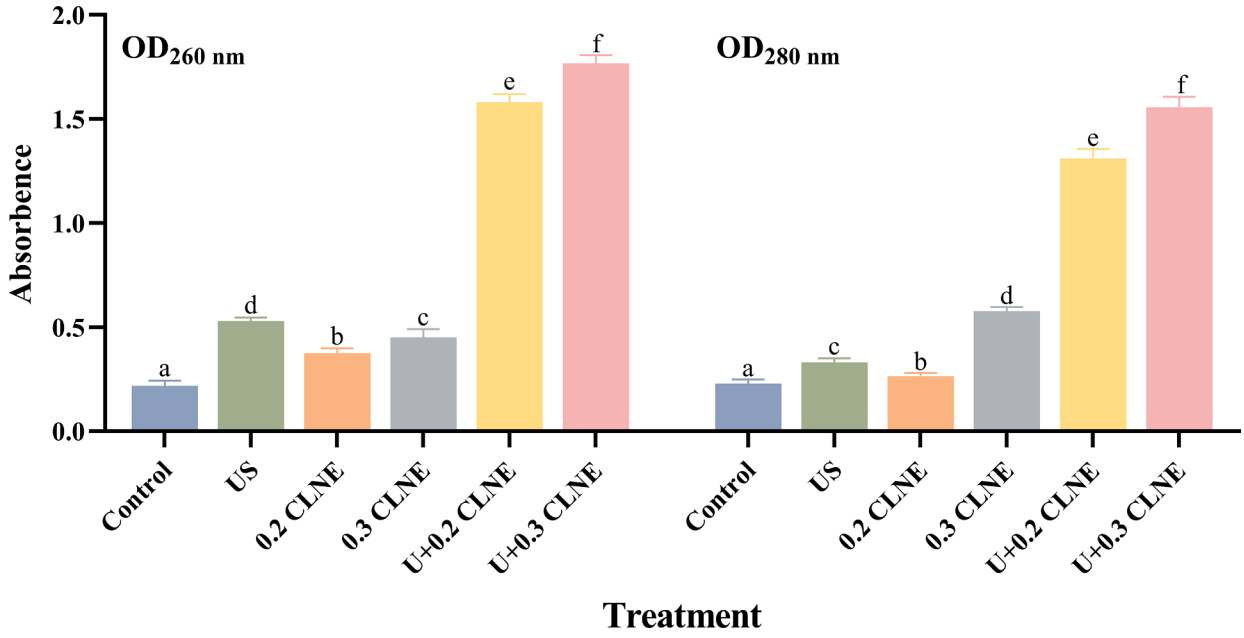

Fig. 3. Nucleic acid and protein release from *S.* Typhimurium cells under different treatments. Different letters indicate statistically significant differences between the treatment groups.

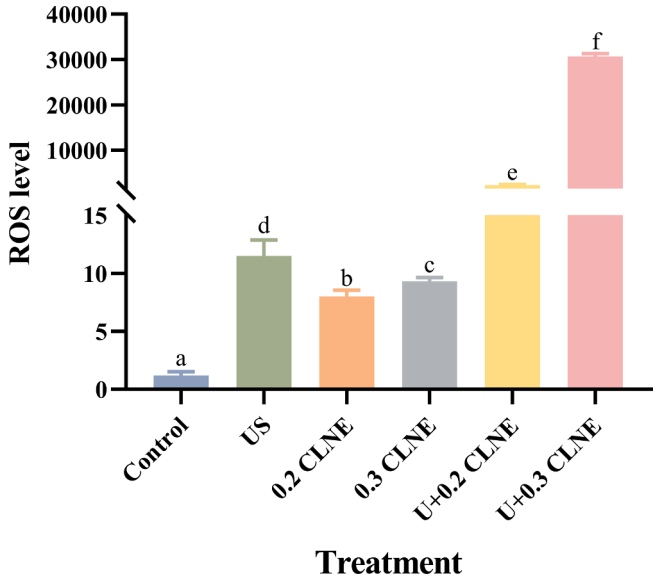

Fig. 4. Intracellular reactive oxygen species (ROS) levels in *S.* Typhimurium upon different treatments. Different letters indicate statistically significant differences between the treatment groups.

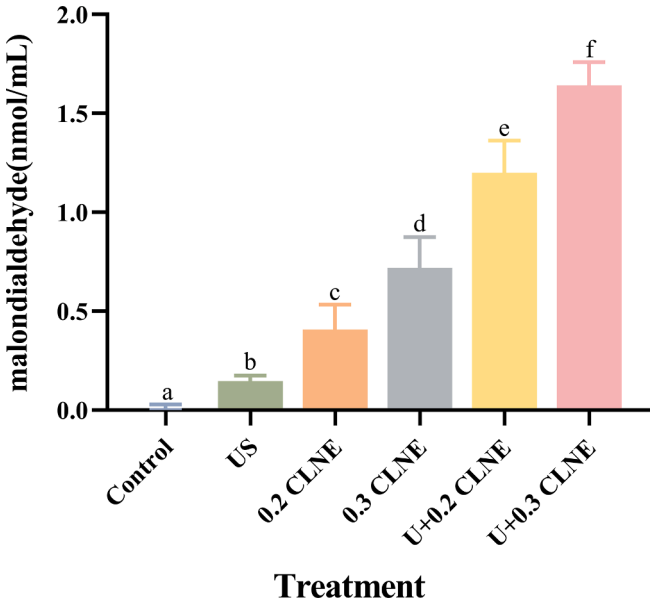

Fig. 5. Extracellular malondialdehyde (MDA) of *S.* Typhimurium under different treatments. Different letters indicate statistically significant differences between the treatment groups.

electron density arrangement in the cytoplasm. After US treatment, a rough cell wall and blurring of the cell membrane were observed in *S.* Typhimurium, along with a larger cellular vacuole space due to aggregation and agglomeration of the cell contents, and similarly, the electron density arrangement within the cell was no longer uniform (Fig. 2B). Treatments with 0.2 and 0.3 mg/mL CLNE exhibited some degree of content agglutination and vacuolation as well as a slight decrease in electron density (Fig. 2C and D). Extremely large vacuolar spaces were observed in the US+CLNE treatment group, with almost complete disintegration of the internal cellular structure, massive loss of cytoplasmic components and imbalance in electron density arrangement (Fig. 2E and F).

3.5. Changes in content leakage of *S.* Typhimurium

$OD_{260\ nm}$ and $OD_{280\ nm}$ values indicating nucleic acids and proteins release during different treatments are shown in Fig. 3. Content leakage was at a low level in the control. The release of nucleic acids and proteins was significantly ($P < 0.05$) elevated after CLNE treatment, with 0.3 mg/mL CLNE resulting in a higher release than 0.2 mg/mL. The US treatment showed a greater ($P < 0.05$) degree of intracellular material leakage compared to the control. The proteins and nucleic acids leakage of *S.* Typhimurium after US+CLNE treatment was significantly ($P < 0.05$) higher than both alone and the sum of both.

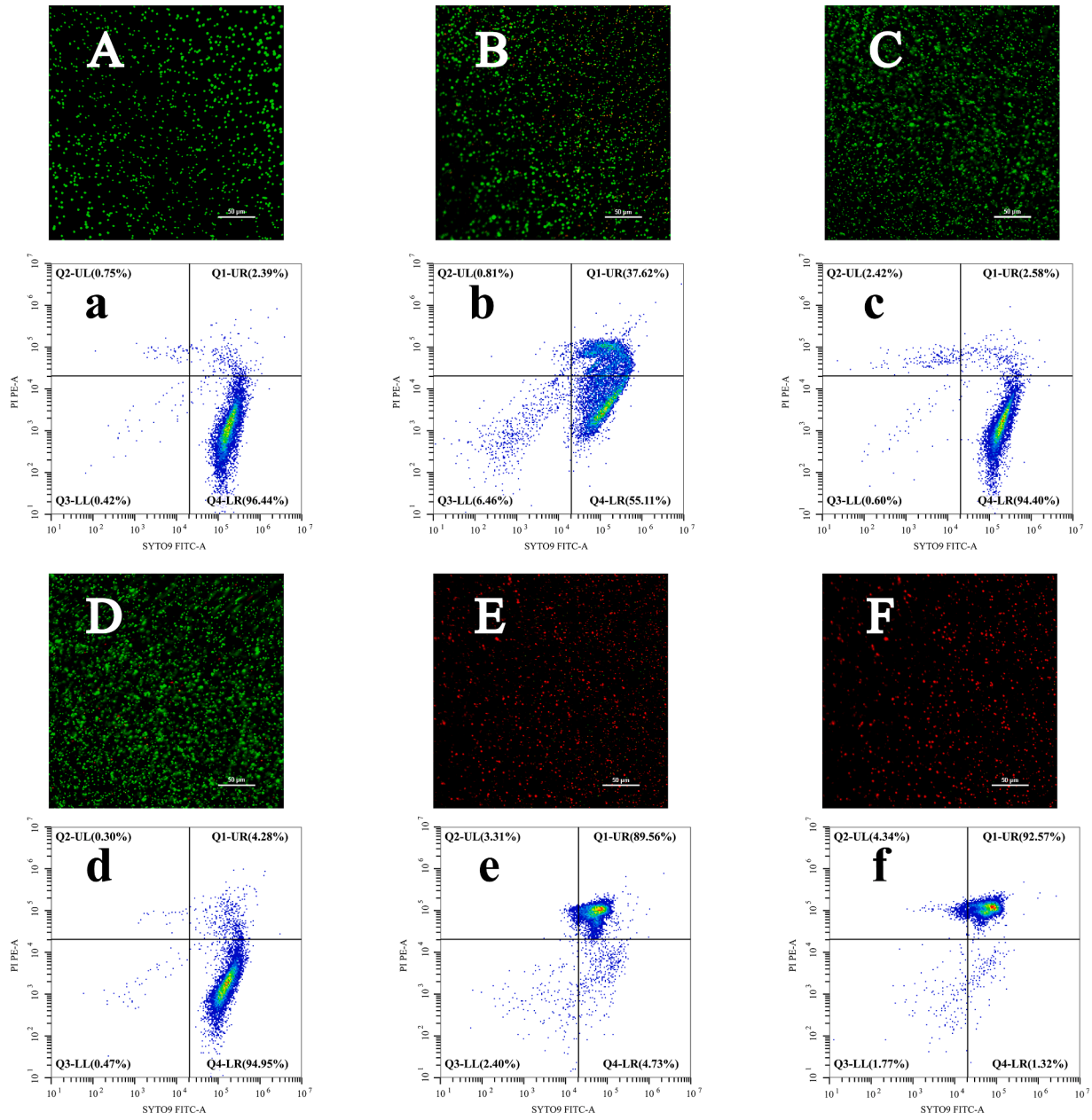

Fig. 6. FCM (a to f) and CLSM (A to F) images of *S*. Typhimurium after different treatments. A, a, Control (untreated); B, b, US (253 W/cm^2, 6 min); C, c, 0.2 mg/mL CLNE; D, d, 0.3 mg/mL CLNE; E, e, US+CLNE (0.2 mg/mL); F, f, US+CLNE (0.3 mg/mL). CLSM, Magnification = 400 ×, bar marker = 50 μm. FCM, Q1: cells with slightly damaged cell membranes. Q2: cells with severely broken cell membranes. Q3: unstained cells or cell debris. Q4: cells with good cell viability and intact morphology.

3.6. Changes in ROS levels in S. Typhimurium

In Fig. 4, the ROS level of untreated *S*. Typhimurium was at a low level. The ROS produced by the action of CLNE was significantly ($P < 0.05$) elevated compared to the control. US alone showed a dramatic increase in ROS over that of healthy *S*. Typhimurium. US+CLNE resulted in significantly ($P < 0.05$) higher changes in ROS levels of *S*. Typhimurium than the respective effects of US and CLNE and the accumulation of values. Specifically, US+0.3 mg/mL CLNE caused a higher elevation of ROS than US+0.2 mg/mL CLNE.

3.7. Changes in extracellular MDA content of S. Typhimurium

As shown in Fig. 5, the control group produced almost no extracellular MDA. The MDA content after US treatment was 8 times higher than that of the control. Treatment with 0.2 mg/mL CLNE significantly ($P < 0.05$) increased the MDA content of *S*. Typhimurium compared to the control. A further increase in MDA production was observed for 0.3 mg/mL CLNE compared to 0.2 mg/mL. For US+CLNE, the MDA content produced was significantly ($P < 0.05$) higher than that of the single treatment and effect superimposed on US and CLNE.

3.8. Changes in cell membrane integrity of S. Typhimurium

The control *S*. Typhimurium showed nearly all green fluorescence (Fig. 6A) and 96.44% intact cell percentage (Fig. 6a), which indicates good cell membrane integrity. For the US treatment, it demonstrated approximately-two-thirds green fluorescence, enhanced red fluorescence (Fig. 6B) and a decrease in the percentage of intact cells to 55.11% (Fig. 6b), demonstrating the significant damage seen in the cell

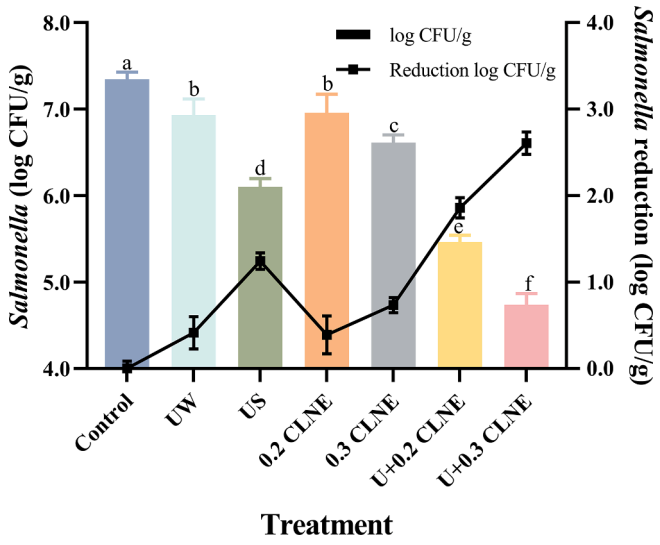

Fig. 7. Decimal reduction of *S*. Typhimurium inoculated on purple kale compared to the control (untreated, Control). Different letters represent statistically significant differences between each microbial treatment group ($P < 0.05$). UW: ultrapure water, US: 253 W/cm^2, 0.2 CLNE: 0.2 mg/mL CLNE, 0.3 CLNE: 0.3 mg/mL CLNE.

Table 3
pH values of purple kale leaves treated with different washing methods and stored at 4°C for 0, 3 and 7 days.

Treatment	Storage time (day)		
	0	3	7
Control	7.31 ± 0.05^{Aa}	7.32 ± 0.04^{Aa}	7.33 ± 0.03^{Aa}
UW	7.33 ± 0.04^{Aa}	7.35 ± 0.03^{Aa}	7.35 ± 0.04^{Aa}
US	7.36 ± 0.05^{Aa}	7.35 ± 0.04^{Aa}	7.37 ± 0.02^{Aa}
0.2 CLNE	7.35 ± 0.03^{Aa}	7.36 ± 0.04^{Aa}	7.38 ± 0.04^{Aa}
0.3 CLNE	7.35 ± 0.04^{Aa}	7.37 ± 0.04^{Aa}	7.39 ± 0.02^{Aa}
U+0.2 CLNE	7.38 ± 0.04^{Aa}	7.38 ± 0.02^{Aa}	7.39 ± 0.02^{Aa}
U+0.3 CLNE	7.38 ± 0.02^{Aa}	7.38 ± 0.05^{Aa}	7.40 ± 0.04^{Aa}

Results are expressed as mean ± SD. Identical uppercase and lowercase letters indicate no statistically significant difference ($P > 0.05$) for any mean in the same column or row. UW: ultrapure water, US: 253 W/cm^2, 0.2 CLNE: 0.2 mg/mL CLNE, 0.3 CLNE: 0.3 mg/mL CLNE. The duration of action was 6 min for all treatment groups.

membrane compared to the control. *S*. Typhimurium showed almost no increase in red fluorescence after 0.2 and 0.3 mg/mL CLNE treatment (Fig. 6C and D), and the percentage of intact cells decreased by only 1.49%–2.04% compared to the control (Fig. 6c and d), indicating that transient treatment with CLNE does not significantly damage the cell membrane. Interestingly, a strong red fluorescence was emitted in the field of view of US+CLNE, and the green fluorescence was close to disappearing (Fig. 6E and F), leaving only 1.32%–4.73% of intact cells (Fig. 6e and f), pointing to a severe damage of the cell membrane and an extremely obvious change of membrane integrity.

3.9. Research on the application of purple kale preservation

3.9.1. Washing effect on S. Typhimurium on kale leaves

The washing effect of ultrapure water (UW), US, CLNE, and US+CLNE on *S*. Typhimurium inoculated on purple kale leaves was evaluated (Fig. 7). The initial counts of *S*. Typhimurium were 7.35 ± 0.08 log CFU/g. Washing of UW and CLNE reduced *S*. Typhimurium by 0.4–0.65 log CFU/g. US and its combined treatment with CLNE have more significant ($P < 0.05$) treatment effect compared to UW and CLNE. Specifically, the US treatment reduced 1.12 log CFU/g. The washing effect of US+CLNE was at least three times greater than that of CLNE, with inoculated *S*. Typhimurium reductions of 1.88–2.56 log CFU/g.

3.9.2. Effects on the physicochemical properties of purple kale leaves

Table 3 shows the varying pH of purple kale leaves from 7.31 to 7.40 during storage. Interestingly, no differences were found between each other.

The color of purple kale leaves is an important parameter to test the change of properties during storage and reflects the intuition of consumers. There were no significant ($P > 0.05$) changes in L*, a*, b* and total color difference (ΔE) of purple kale leaves during storage (Table 4 Fig. 8), indicating that US and US+CLNE do not affect the color of purple kale during fresh cutting and storage.

The changes in hardness of purple kale leaves during storage are responded to in Table 5. The different treatments of 6 min did not affect the hardness of the leaves and no time correlation was found during the three time periods of storage.

4. Discussion

In the present study, we prepared CLNE using ultrasonic emulsification, which had an average particle size of 29.4 ± 0.1 nm, a PDI of 0.291 ± 0.006, and a zeta potential of -18.93 ± 1.39 mV (Table 5). Similarly, Zamaniahari et al [30] reported an average particle size of 51.46 nm, PDI of 0.296 and zeta potential of -13.2 mV for peppermint essential oil nanoemulsion prepared by ultrasonication. This indicates that CLNE is a small particle size and well dispersed nanoemulsion.

US (115–253 W/cm^2, 2–8 min) treatment showed a limited killing effect on *S*. Typhimurium (Table 2). Similarly, Li et al [31] reported only 0.47–0.52 log CFU/mL reduction in the number of *Staphylococcus aureus* after 8 min of 60 W/cm^2 ultrasonic treatment. Low-frequency ultrasound achieves sterilization through mechanical, thermal, and cavitation effects [32]. We speculate that the difference in bactericidal effect may be related to bacterial species, ultrasound parameters, and ultrasound probe location. Nanoemulsification has shown an optimistic trend by virtue of the important advantage of encapsulating bioactive lipophilic components and enhancing their activity [33]. Similarly, the fennel extract nanoemulsion prepared by Ghazy et al [34] significantly ($P < 0.05$) increased the inhibition circle of *Yersinia enterocolitica*. In our study, 0.2 and 0.3 mg/mL CLNE only reduced the population level of *S*. Typhimurium by 0.23–0.57 log CFU/mL. However, US+CLNE demonstrated a stronger bactericidal effect. The combined treatment of US (253 W/cm^2) and 0.3 mg/mL exhibited a bactericidal effect that was 6.69 log CFU/mL greater than the superposition of the two single treatments. Similarly, Dolan et al [16] found that *Listeria innocua* decreased by 1 log CFU/mL after US (20 kHz) treatment alone and no antimicrobial effect was detected with 40 mM ZnO, but US combined with ZnO decreased the bacterial load by 5 log CFU/mL. Yoon et al [35] reported that *Listeria monocytogenes* treated with US (40 kHz) in combination with 3% malic acid and 0.1% lactobacillus peptide decreased to below the limit of detection in oyster mushrooms. Therefore, the combination of low-power ultrasound and CLNE for a short time can achieve significant sterilization effects.

The detection of absorption peaks at 260 and 280 nm represents the leakage of nucleic acids and proteins from the bacterial cytoplasm, which was used to indirectly determine changes in membrane integrity [36]. In the current study, $OD_{260\ nm}$ and $OD_{280\ nm}$ of *S*. Typhimurium medium increased significantly ($P < 0.05$) after different treatments, and the US+CLNE increased particularly strongly (Fig. 3). Similarly, Sun et al [37] found that US and chlorogenic acid showed strong synergistic effects on the release of cellular components from *Pseudomonas fluorescens*. The results of Sun et al [38] showed that the combined treatment with ultrasound and microtherm effectively promoted protein, nucleic acid and ATP leakage in *Klebsiella pneumoniae*, indicating cell membrane damage. Our results suggested that US+CLNE acts on the cytoplasmic membrane in its antimicrobial action, causing irreversible damage, which leads to loss of macromolecular contents and cell death.

Table 4
Changes in the surface color of purple kale leaves after treatment with different washing methods during storage at 4°C for 0, 3 and 7 days.

Colour parameter	Storage time (day)	Treatment						
		Control	UW	US	0.2 CLNE	0.3 CLNE	U+0.2 CLNE	U+0.3 CLNE
L*	0	37.4 ± 0.76^{Aa}	37.46 ± 0.52^{Aa}	37.54 ± 0.46^{Aa}	37.51 ± 0.54^{Aa}	37.15 ± 0.41^{Aa}	37.35 ± 0.79^{Aa}	37.41 ± 0.47^{Aa}
	3	37.66 ± 0.55^{Aa}	37.26 ± 0.32^{Aa}	37.29 ± 0.70^{Aa}	37.42 ± 0.65^{Aa}	37.56 ± 0.70^{Aa}	37.46 ± 0.34^{Aa}	37.04 ± 0.29^{Aa}
	7	37.66 ± 0.78^{Aa}	37.22 ± 0.49^{Aa}	37.54 ± 0.69^{Aa}	37.68 ± 0.63^{Aa}	37.54 ± 0.73^{Aa}	37.45 ± 0.14^{Aa}	37.42 ± 0.11^{Aa}
a*	0	25.54 ± 0.46^{Aa}	26.19 ± 0.74^{Aa}	25.57 ± 0.76^{Aa}	25.92 ± 0.76^{Aa}	25.83 ± 0.51^{Aa}	25.7 ± 0.81^{Aa}	25.99 ± 0.83^{Aa}
	3	25.8 ± 0.75^{Aa}	25.83 ± 0.66^{Aa}	25.59 ± 0.36^{Aa}	25.97 ± 0.79^{Aa}	25.74 ± 0.36^{Aa}	25.85 ± 0.39^{Aa}	26.05 ± 0.32^{Aa}
	7	25.46 ± 0.58^{Aa}	25.95 ± 0.49^{Aa}	25.63 ± 0.54^{Aa}	25.29 ± 0.42^{Aa}	25.33 ± 0.48^{Aa}	25.26 ± 0.47^{Aa}	25.77 ± 0.65^{Aa}
b*	0	-11.85 ± 0.71^{Aa}	-11.43 ± 0.66^{Aa}	-11.66 ± 0.79^{Aa}	-11.42 ± 0.71^{Aa}	-11.35 ± 0.41^{Aa}	-11.71 ± 0.30^{Aa}	-11.38 ± 0.36^{Aa}
	3	-11.27 ± 0.68^{Aa}	-11.58 ± 0.52^{Aa}	-11.41 ± 0.35^{Aa}	-11.34 ± 0.55^{Aa}	-11.18 ± 0.48^{Aa}	-11.73 ± 0.62^{Aa}	-11.49 ± 0.15^{Aa}
	7	-11.26 ± 0.70^{Aa}	-11.43 ± 0.35^{Aa}	-11.23 ± 0.41^{Aa}	-11.26 ± 0.24^{Aa}	-11.76 ± 0.54^{Aa}	-11.77 ± 0.27^{Aa}	-11.42 ± 0.44^{Aa}
ΔE	0	1.55 ± 0.76^{Aa}	1.62 ± 0.23^{Aa}	1.66 ± 0.50^{Aa}	1.66 ± 0.41^{Aa}	1.70 ± 0.41^{Aa}	1.63 ± 0.64^{Aa}	1.65 ± 0.29^{Aa}
	3	1.71 ± 0.38^{Aa}	1.58 ± 0.42^{Aa}	1.68 ± 0.56^{Aa}	1.73 ± 0.40^{Aa}	1.69 ± 0.38^{Aa}	1.56 ± 0.51^{Aa}	1.57 ± 0.18^{Aa}
	7	1.88 ± 0.39^{Aa}	1.56 ± 0.46^{Aa}	1.71 ± 0.47^{Aa}	1.74 ± 0.43^{Aa}	1.70 ± 0.34^{Aa}	1.55 ± 0.36^{Aa}	1.54 ± 0.38^{Aa}

Results are expressed as mean ± SD. Identical uppercase and lowercase letters indicate no statistically significant difference ($P > 0.05$) for any mean in the same column or row. UW: ultrapure water, US: 253 W/cm^2, 0.2 CLNE: 0.2 mg/mL CLNE, 0.3 CLNE: 0.3 mg/mL CLNE. The duration of action was 6 min for all treatment groups.

ROS play an important role in cell signaling and tissue homeostasis [39]. High levels of ROS attack the cell membrane and induce cell death [40]. US+CLNE caused an overproduction of ROS in *S*. Typhimurium compared to the control (Fig. 4). Similarly, Pan et al [41] found that short ultrasound-assisted plasma increased ROS levels in *L. monocytogenes*, possibly because the treatment promoted intracellular oxidative stress. Our results showed that US+CLNE caused oxidative stress and increased intracellular ROS levels in *S*. Typhimurium, which further damaged the cytoplasmic membrane and accelerated bacterial death.

MDA is the main product of peroxidation of membrane lipids due to oxidative stress, and its content indicates the intensity and rate of lipid peroxidation, which indirectly reflects the extent of cellular peroxidative damage [42,43]. The extracellular MDA content of *S*. Typhimurium under US+CLNE treatment was significantly ($P < 0.05$) higher than that of the single treatment. Similarly, Liu et al [44] showed that carvacrol-loaded nanoemulsions caused elevated MDA levels in *Escherichia coli* and *S. aureus*. This was consistent with the treatment trend of ROS (Fig. 5). By the measurement results of ROS, US+CLNE caused an increase in ROS levels and induced further peroxidation of membrane lipids.

In this study, changes in membrane integrity of *S*. Typhimurium were characterized and quantified using CLSM and FCM, respectively. SYTO 9 can rapidly penetrate the cell membrane of any cell and bind to nucleic acids, and cells appear green fluorescent; PI can only bind nucleic acids through damaged cell membranes, thus staining the cells red [45]. US+CLNE showed a higher proportion of red fluorescent regions and membrane-broken cells than both treatments alone, indicating a stronger disruption of cell membrane integrity with US+CLNE (Fig. 6). Similarly, Sun et al [46] observed that almost all *Salmonella enteritidis* was stained red by PI after ultrasound combined with chlorogenic acid treatment. Shu et al [47] detected a 2.50% higher percentage of membrane disruption in *S. aureus* by combined ultrasound and MEL-A treatment compared to the control group, which was due to the pores created in the cell membrane by ultrasound cavitation exacerbating the damage to the plasma membrane by MEL-A. Stable ultrasonic cavitation leads to the creation of pores in the bacterial cell membrane, causing a change in properties including enhanced permeability of the bacterial cell membrane, which facilitates the penetration of the antimicrobial agent [48]. Therefore, a potential mechanism for the disruption of membrane integrity caused by US+CLNE could be that the impact of ultrasound-generated cavitation bubbles upon rupture created pores in the cell membrane. It drives CLNE to a greater extent into the interior of the cell, thus causing a change in intracellular tissue homeostasis and contributing to a greater degree of damage to membrane integrity.

In this paper, morphological and ultrastructural changes of *S*. Typhimurium were observed using FESEM & TEM. Compared to the slight desiccation with partial loss of matrix caused by US and CLNE treatment alone, US+CLNE demonstrated a greater degree of cell fragmentation and internal vacuolar space (Figs. 1 and 2). Krishnamoorthy et al [49] found that *Cleome viscosa* essential oil nanoemulsion caused loss of linear structure and surface ruffling in *Candida albicans*. TEM images of different ultrasound times by Li et al [31] showed fuzzy outer membranes and rough or even ruptured cell walls of *E. coli*, elaborating ultrasound uses the outer membrane of Gram-negative bacteria as the main target. Ultrasound can improve the permeability of cell membranes through the acoustic perforation effect, that is, cells form transient pores in the cell membrane via the shear force of acoustic cavitation [50]. Guo et al [51] found that ultrasound combined with thyme essential oil nanoemulsion (TEON) caused rupture of *E. coli* cells and loss of contents. He et al [21] showed in a subsequent study that pores in the membrane produced by ultrasonic cavitation led to permeabilization of the cells, which in turn increased the sensitivity of *E. coli* to TEON. Thus, FESEM & TEM and CLSM & FCM were linked to obtain that ultrasound uses acoustic cavitation to create pores in the cytoplasmic membrane and CLNE further acts to destroy the integrity of the cell membrane, cell matrix loss, cell drying and shrinkage or even death.

In the current study, the washing effect of US+CLNE against *S*. Typhimurium was stronger than the single treatment of both (Fig. 7). Similarly, Park et al [52] showed that ultrasound (40 kHZ) treatment of fresh-cut chicory for 3 min reduced surface *E. coli* by 0.40 log CFU/g. Combination of US with cinnamon leaf oil emulsion (CLB, CLC) decreased *E. coli* to 1.46–1.60 log CFU/g. High concentrations of EOs may accentuate the sensory disadvantage to fresh-cut foods [53]. Nanoemulsions play an important role in extending the shelf life or improving the quality of different foods, such as inhibition of bacteria, reduction of weight, color changes and oxidation reactions of different foods [54]. CLNE did not cause apparent changes in the color and hardness of purple kale (Tables 4 and 5). Similarly, Ru et al [55] reported that no softening upon storage was observed in fresh-cut melons treated with laurel essential oil nanoemulsion. In our results, US+CLNE had no effective effect on the total color difference, hardness, and pH of purple kale (Tables 3–5). Similarly, Wu et al [56] observed a similar trend and reported that the application of US combined with NaClO effectively reduced the natural microbiota on the surface of cabbage as

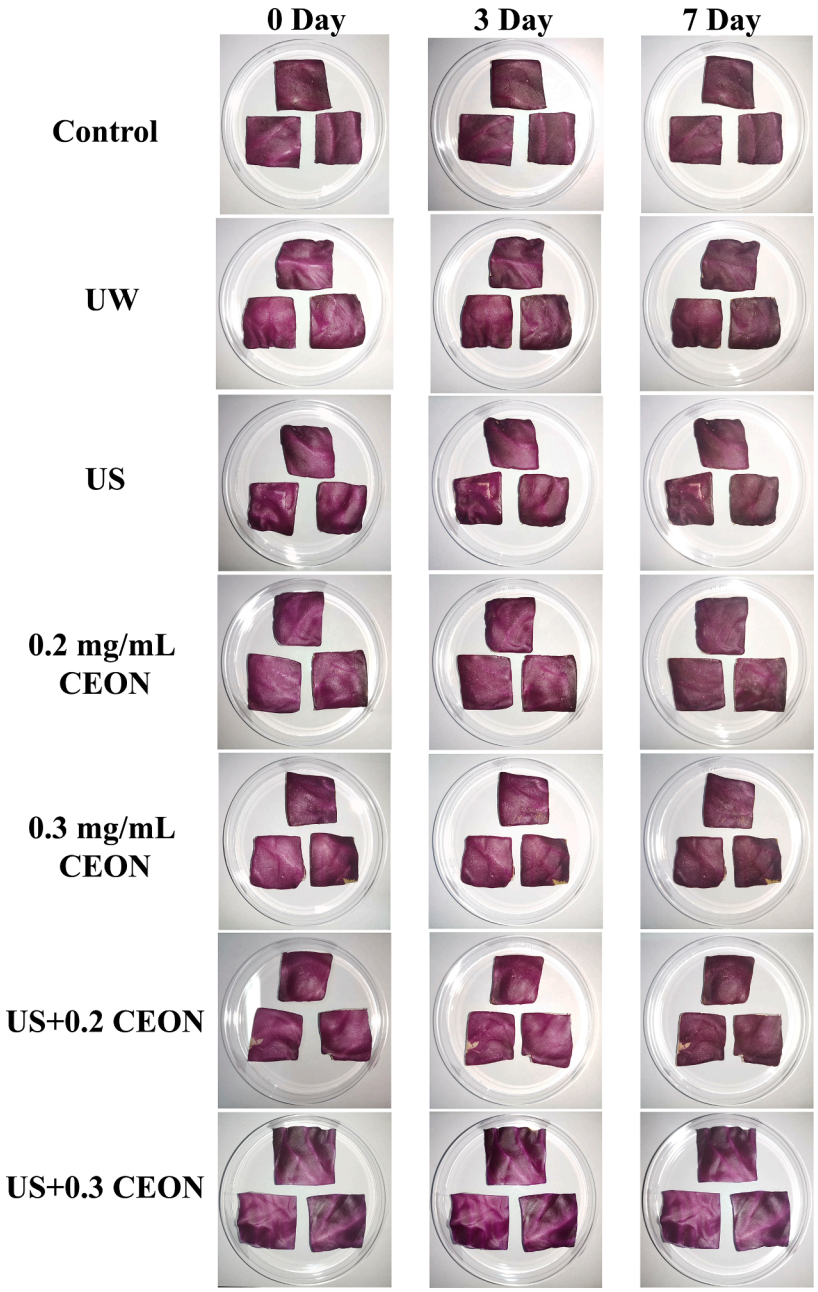

Fig. 8. Effect of different washing methods on purple kale leaves during storage. UW: ultrapure water, US: 253 W/cm^2, 0.2 CLNE: 0.2 mg/mL CLNE, 0.3 CLNE: 0.3 mg/mL CLNE.

well as the degradation of chlorophyll inside cabbage. He et al [57] reported a significant reduction of *E. coli* on the surface of cherry tomatoes when treated with US+TEON for 3 min, with changes in color and hardness of cherry tomatoes within acceptable range. This study showed that the use of CLNE in combination with ultrasound at low power levels for a short period of time can be considered as an appropriate treatment to improve the washing effect of *S*. Typhimurium as well as to maintain the physicochemical properties of purple kale.

5. Conclusion

Taken together, the citral nanoemulsions prepared by ultrasonic emulsification had a small particle size distribution and good dispersion in this research. The killing effect of US and CLNE treatment alone on *S*. Typhimurium was limited, and US+CLNE had a significant synergistic effect on the reduction of the population of *S*. Typhimurium. The mechanism may involve that ultrasound accelerates the formation of membrane perforations through acoustic cavitation, allowing CLNE to enter intracellularly more easily to enhance its antimicrobial activity. Synergistic effects include disruption of the cell morphology and membranes of *S*. Typhimurium, leading to efflux of cellular components. In addition, stimulation of US+CLNE induced cell death in *S*. Typhimurium by causing excessive production of ROS and MDA, which effectively altered membrane integrity and permeability. The study obviously enhanced the effectiveness of washing against *S*. Typhimurium inoculated on the surface of purple kale, and effectively maintained the quality characteristics of purple kale during storage.

In conclusion, the combination of ultrasound and CLNE is a method that can substantially increase antimicrobial activity while having great potential for application in the sterilization of fresh-cut foods.

Table 5
Hardness (kg) of purple kale leaves after treatment with different washing methods during storage at 4°C for 0, 3 and 7 days.

Treatment	Storage time (day)		
	0	3	7
Control	1.57 ± 0.15^{Aa}	1.54 ± 0.26^{Aa}	1.62 ± 0.28^{Aa}
UW	1.47 ± 0.08^{Aa}	1.45 ± 0.24^{Aa}	1.58 ± 0.15^{Aa}
US	1.60 ± 0.14^{Aa}	1.55 ± 0.24^{Aa}	1.63 ± 0.38^{Aa}
0.2 CLNE	1.49 ± 0.11^{Aa}	1.53 ± 0.12^{Aa}	1.67 ± 0.20^{Aa}
0.3 CLNE	1.65 ± 0.25^{Aa}	1.63 ± 0.23^{Aa}	1.70 ± 0.28^{Aa}
U+0.2 CLNE	1.45 ± 0.10^{Aa}	1.40 ± 0.12^{Aa}	1.59 ± 0.35^{Aa}
U+0.3 CLNE	1.56 ± 0.11^{Aa}	1.57 ± 0.20^{Aa}	1.84 ± 0.25^{Aa}

Results are expressed as mean ± SD. Identical uppercase and lowercase letters indicate no statistically significant difference ($P > 0.05$) for any mean in the same column or row. UW: ultrapure water, US: 253 W/cm^2, 0.2 CLNE: 0.2 mg/mL CLNE, 0.3 CLNE: 0.3 mg/mL CLNE. The duration of action was 6 min for all treatment groups.

CRediT authorship contribution statement

Hui Yang: Conceptualization, Investigation, Project administration, Writing – original draft. **Luyi Song:** Methodology, Data curation, Writing – review & editing, Visualization. **Peiwen Sun:** Resources, Data curation, Investigation, Investigation, Validation, Resources. **Ruiying Su:** Resources, Formal analysis, Data curation. **Shuqi Wang:** Formal analysis, Data curation. **Shuai Cheng:** Writing – review & editing, Visualization, Formal analysis. **Xiangjun Zhan:** Project administration. **Xin Lü:** Supervision. **Xiaodong Xia:** Visualization, Writing – review & editing. **Chao Shi:** Project administration, Supervision, Funding acquisition, Writing – review & editing.

Declaration of Competing Interest

The authors declare that they have no known competing financial interests or personal relationships that could have appeared to influence the work reported in this paper.

Acknowledgments

This work was supported by the National Natural Science Foundation of China (32272445 and 31801659) and the class General Financial Grant from the Shaanxi Postdoctoral Science Foundation (2018BSHEDZZ150). Meanwhile, we thank Dr. Zhang Guoyun (State Key Laboratory of Crop Stress Biology for Arid Areas, Northwest A&F University, Yangling, China) for FESEM experimental assistance.

References

[1] D. Millan-Sango, E. Garroni, C. Farrugia, J.F. Van Impe, V. Valdramidis, Determination of the efficacy of ultrasound combined with essential oils on the decontamination of *Salmonella* inoculated lettuce leaves, LWT Food Sci. Technol. 73 (2016) 80–87, https://doi.org/10.1016/j.lwt.2016.05.039.

[2] O. Ehuwa, A.K. Jaiswal, S. Jaiswal, *Salmonella*, food safety and food handling practices, Foods 10 (5) (2021) 907, https://doi.org/10.3390/foods10050907.

[3] I. Kljujev, V. Raicevic, B. Vujovic, M. Rothballer, M. Schmid, *Salmonella* as an endophytic colonizer of plants - A risk for health safety vegetable production, Microb. Pathog. 115 (2018) 199–207, https://doi.org/10.1016/j.micpath.2017.12.020.

[4] A.L.A. Duarte, D.K.A. do Rosário, S.B.S. Oliveira, H.L.S. de Souza, R.V. de Carvalho, J.C.S. Carneiro, P.I. Silva, P.C. Bernardes, Ultrasound improves antimicrobial effect of sodium dichloroisocyanurate to reduce *Salmonella* Typhimurium on purple cabbage, Int. J. Food Microbiol. 269 (2018) 12–18.

[5] K.-M. Park, H.-J. Kim, J.-Y. Choi, M. Koo, Antimicrobial effect of acetic acid, sodium hypochlorite, and thermal treatments against psychrotolerant *Bacillus cereus* group isolated from lettuce (*Lactuca sativa* L.), Foods 10 (9) (2021) 2165, https://doi.org/10.3390/foods10092165.

[6] D.K.A. Rosario, A.L.A. Duarte, M.C.M. Madalao, M.C. Libardi, L.J.Q. Teixeira, C. A. Conte-Junior, P.C. Bernardes, Ultrasound improves antimicrobial effect of sodium hypochlorite and instrumental texture on fresh-cut yellow melon, J Food Qual. 2018 (2018) 1–6.

[7] N. Hatanaka, S.P. Awasthi, H. Goda, H. Kawata, Y. Uchino, T. Kubo, S. Aoki, A. Hinenoya, S. Yamasaki, Chlorous acid is a more potent antibacterial agent than sodium hypochlorite against *Campylobacter*, Food Control 111 (2020), 107046, https://doi.org/10.1016/j.foodcont.2019.107046.

[8] V. Ryu, D.J. McClements, M.G. Corradini, L. McLandsborough, Effect of ripening inhibitor type on formation, stability, and antimicrobial activity of thyme oil nanoemulsion, Food Chem. 245 (2018) 104–111, https://doi.org/10.1016/j.foodchem.2017.10.084.

[9] X. Huang, Y. Lao, Y. Pan, Y. Chen, H. Zhao, L. Gong, N. Xie, C.-H. Mo, Synergistic antimicrobial effectiveness of plant essential oil and its application in seafood preservation: a review, Molecules 26 (2) (2021) 307, https://doi.org/10.3390/molecules26020307.

[10] S. Burt, Essential oils: their antibacterial properties and potential applications in foods—a review, Int. J. Food Microbiol. 94 (3) (2004) 223–253, https://doi.org/10.1016/j.ijfoodmicro.2004.03.022.

[11] X. Fu, Y. Gao, W. Yan, Z. Zhang, S. Sarker, Y. Yin, Q. Liu, J. Feng, J. Chen, Preparation of eugenol nanoemulsions for antibacterial activities, RSC Adv. 12 (6) (2022) 3180–3190, https://doi.org/10.1039/d1ra08184e.

[12] B.D. da Silva, D.K.A. do Rosário, D.A. Weitz, C.A. Conte-Junior, Essential oil nanoemulsions: Properties, development, and application in meat and meat products, Trends Food Sci, Tech. 121 (2022) 1–13.

[13] C. Solans, P. Izquierdo, J. Nolla, N. Azemar, M.J. Garcia-Celma, Nano-emulsions, Curr. Opin. Colloid Interface Sci. 10 (3–4) (2005) 102–110, https://doi.org/10.1016/j.cocis.2005.06.004.

[14] H.D. Silva, M.Â. Cerqueira, A.A. Vicente, Nanoemulsions for food applications: development and characterization, Food Bioproc. Tech. 5 (3) (2012) 854–867, https://doi.org/10.1007/s11947-011-0683-7.

[15] M. Erriu, C. Blus, S. Szmukler-Moncler, S. Buogo, R. Levi, G. Barbato, D. Madonnaripa, G. Denotti, V. Piras, G. Orrù, Microbial biofilm modulation by ultrasound: Current concepts and controversies, Ultrason. Sonochem. 21 (1) (2014) 15–22, https://doi.org/10.1016/j.ultsonch.2013.05.011.

[16] H.L. Dolan, L.J. Bastarrachea, R.V. Tikekar, Inactivation of *Listeria innocua* by a combined treatment of low-frequency ultrasound and zinc oxide, LWT Food Sci. Technol. 88 (2018) 146–151, https://doi.org/10.1016/j.lwt.2017.10.008.

[17] M. Zupanc, Ž. Pandur, T.S. Perdih, D. Stopar, M. Petkovšek, M. Dular, Effects of cavitation on different microorganisms: The current understanding of the mechanisms taking place behind the phenomenon. A review and proposals for further research, Ultrason. Sonochem. 57 (2019) 147–165, https://doi.org/10.1016/j.ultsonch.2019.05.009.

[18] J. Dai, M. Bai, C. Li, H. Cui, L. Lin, Advances in the mechanism of different antibacterial strategies based on ultrasound technique for controlling bacterial contamination in food industry, Trends Food Sci. Tech. 105 (2020) 211–222, https://doi.org/10.1016/j.tifs.2020.09.016.

[19] A. Prakash, R. Baskaran, V. Vadivel, Citral nanoemulsion incorporated edible coating to extend the shelf life of fresh cut pineapples, LWT Food Sci. Technol. 118 (2020), 108851, https://doi.org/10.1016/j.lwt.2019.108851.

[20] L. Guo, Y. Sun, Y. Zhu, B. Wang, L. Xu, M. Huang, Y. Li, J. Sun, The antibacterial mechanism of ultrasound in combination with sodium hypochlorite in the control of *Escherichia coli*, Food Res. Int. 129 (2020), 108887, https://doi.org/10.1016/j.foodres.2019.108887.

[21] Q. He, D. Liu, M. Ashokkumar, X. Ye, T.Z. Jin, M. Guo, Antibacterial mechanism of ultrasound against *Escherichia coli*: Alterations in membrane microstructures and properties, Ultrason. Sonochem. 73 (2021), 105509, https://doi.org/10.1016/j.ultsonch.2021.105509.

[22] S. Liao, Y. Zhang, X. Pan, F. Zhu, C. Jiang, Q. Liu, Z. Cheng, G. Dai, G. Wu, L. Wang, Antibacterial activity and mechanism of silver nanoparticles against multidrug-resistant *Pseudomonas aeruginosa*, Int. J. Nanomed. 14 (2019) 1469–1487, https://doi.org/10.2147/IJN.S191340.

[23] L. Zhang, M. Zhang, A.S. Mujumdar, K. Liu, Antibacterial mechanism of ultrasound combined with sodium hypochlorite and their application in pakchoi (*Brassica campestris* L. ssp. *chinensis*), J. Sci. Food Agric. 102 (11) (2022) 4685–4696, https://doi.org/10.1002/jsfa.11829.

[24] D. Díaz-García, P.R. Ardiles, M. Díaz-Sánchez, I. Mena-Palomo, I. Del Hierro, S. Prashar, A. Rodríguez-Diéguez, P.L. Páez, S. Gómez-Ruiz, Copper-functionalized nanostructured silica-based systems: Study of the antimicrobial applications and ROS generation against gram positive and gram negative bacteria, J. Inorg. Biochem. 203 (2020), 110912, https://doi.org/10.1016/j.jinorgbio.2019.110912.

[25] J. Cao, H. Liu, Y. Wang, X. He, H. Jiang, J. Yao, F. Xia, Y. Zhao, X. Chen, Antimicrobial and antivirulence efficacies of citral against foodborne pathogen *Vibrio parahaemolyticus* RIMD2210633, Food Control 120 (2021), 107507, https://doi.org/10.1016/j.foodcont.2020.107507.

[26] L. Tian, X. Wang, R. Liu, D. Zhang, X. Wang, R. Sun, W. Guo, S. Yang, H. Li, G. Gong, Antibacterial mechanism of thymol against *Enterobacter sakazakii*, Food Control 123 (2021), 107716, https://doi.org/10.1016/j.foodcont.2020.107716.

[27] N.G. Nieto-Velázquez, A.A. Gomez-Valdez, M. González-Ávila, J. Sánchez-Navarrete, J.D. Toscano-Garibay, N.J. Ruiz-Pérez, Preliminary study on citrus oils antibacterial activity measured by flow cytometry: a step-by-step development, Antibiotics 10 (10) (2021) 1218, https://doi.org/10.3390/antibiotics10101218.

[28] J.-H. Kang, S.-J. Park, J.-B. Park, K.B. Song, Surfactant type affects the washing effect of cinnamon leaf essential oil emulsion on kale leaves, Food Chem. 271 (2019) 122–128, https://doi.org/10.1016/j.foodchem.2018.07.203.

[29] K. Fan, M. Zhang, F. Jiang, Ultrasound treatment to modified atmospheric packaged fresh-cut cucumber: Influence on microbial inhibition and storage quality, Ultrason. Sonochem. 54 (2019) 162–170, https://doi.org/10.1016/j.ultsonch.2019.02.003.

[30] S. Zamaniahari, A. Jamshidi, M.-H. Moosavy, S.A. Khatibi, Preparation and evaluation of *Mentha spicata* L. essential oil nanoemulsion: physicochemical properties, antibacterial activity against foodborne pathogens and antioxidant

properties, Food Measure. 16 (4) (2022) 3289–3300, https://doi.org/10.1007/s11694-022-01436-9.
[31] J. Li, J. Ahn, D. Liu, S. Chen, X. Ye, T. Ding, C.A. Elkins, Evaluation of ultrasound-induced damage to *Escherichia coli* and *Staphylococcus aureus* by flow cytometry and transmission electron microscopy, Appl. Environ. Microb. 82 (6) (2016) 1828–1837, https://doi.org/10.1128/AEM.03080-15.
[32] K. Yan, T. Yang, J. Xu, L. Dong, J. Wang, Y. Cai, Synergistic effect of low-frequency ultrasound and antibiotics on the treatment of *Klebsiella pneumoniae* pneumonia in mice, Microb. Biotechnol. 15 (11) (2022) 2819–2830, https://doi.org/10.1111/1751-7915.14134.
[33] A. Rezaei, M. Fathi, S.M. Jafari, Nanoencapsulation of hydrophobic and low-soluble food bioactive compounds within different nanocarriers, Food Hydrocoll. 88 (2019) 146–162, https://doi.org/10.1016/j.foodhyd.2018.10.003.
[34] O.A. Ghazy, M.T. Fouad, H.H. Saleh, A.E. Kholif, T.A. Morsy, Ultrasound-assisted preparation of anise extract nanoemulsion and its bioactivity against different pathogenic bacteria, Food Chem. 341 (2021), 128259, https://doi.org/10.1016/j.foodchem.2020.128259.
[35] J.-H. Yoon, D.-Y. Jeong, S.-B. Lee, S. Choi, M.-I. Jeong, S.-Y. Lee, S.-R. Kim, Decontamination of *Listeria monocytogenes* in king oyster mushrooms (*Pleurotus eryngii*) by combined treatments with organic acids, nisin, and ultrasound, LWT Food Sci. Technol. 144 (2021), 111207, https://doi.org/10.1016/j.lwt.2021.111207.
[36] P. Sharma, J. Wichaphon, W. Klangpetch, Antimicrobial and antioxidant activities of defatted *Moringa oleifera* seed meal extract obtained by ultrasound-assisted extraction and application as a natural antimicrobial coating for raw chicken sausages, Int. J. Food Microbiol. 332 (2020), 108770, https://doi.org/10.1016/j.ijfoodmicro.2020.108770.
[37] J. Sun, L. Huang, Z. Sun, D. Wang, F. Liu, L. Du, D. Wang, Combination of ultrasound and chlorogenic acid for inactivation of planktonic and biofilm cells of *Pseudomonas fluorescens*, Food Res. Int. 155 (2022), 111009, https://doi.org/10.1016/j.foodres.2022.111009.
[38] J. Sun, D. Wang, J. Zhang, Z. Sun, Q. Xiong, F. Liu, Antibacterial and antibiofilm effect of ultrasound and mild heat against a multidrug-resistant *Klebsiella pneumoniae* stain isolated from meat of yellow-feathered chicken, Foodborne Pathog. Dis. 19 (1) (2022) 70–79, https://doi.org/10.1089/fpd.2021.0025.
[39] C.A. Ferreira, D. Ni, Z.T. Rosenkrans, W. Cai, Scavenging of reactive oxygen and nitrogen species with nanomaterials, Nano Res. 11 (10) (2018) 4955–4984, https://doi.org/10.1007/s12274-018-2092-y.
[40] L.-J. Su, J.-H. Zhang, H. Gomez, R. Murugan, X. Hong, D. Xu, F. Jiang, Z.-Y. Peng, Reactive oxygen species-induced lipid peroxidation in apoptosis, autophagy, and ferroptosis, Oxidative Med. Cell. Longev. 2019 (2019) 5080843, https://doi.org/10.1155/2019/5080843.
[41] Y. Pan, Y. Zhang, J.-H. Cheng, D.-W. Sun, Inactivation of *Listeria Monocytogenes* at various growth temperatures by ultrasound pretreatment and cold plasma, LWT Food Sci. Technol. 118 (2020), 108635, https://doi.org/10.1016/j.lwt.2019.108635.
[42] M. Kheiry, M. Dianat, M. Badavi, S.A. Mard, V. Bayati, p-Coumaric acid attenuates lipopolysaccharide-induced lung inflammation in rats by scavenging ROS production: an *in vivo* and *in vitro* study, Inflammation 42 (6) (2019) 1939–1950, https://doi.org/10.1007/s10753-019-01054-6.
[43] B. Xia, Q. Sui, X. Sun, Q. Han, B. Chen, L. Zhu, K. Qu, Ocean acidification increases the toxic effects of TiO_2 nanoparticles on the marine microalga *Chlorella vulgaris*, J. Hazard. Mater. 346 (2018) 1–9, https://doi.org/10.1016/j.jhazmat.2017.12.017.
[44] Q. Liu, Z. Wang, A. Mukhamadiev, J. Feng, Y. Gao, X. Zhuansun, R. Han, Y. Chong, S.M. Jafari, Formulation optimization and characterization of carvacrol-loaded nanoemulsions: *In vitro* antibacterial activity/mechanism and safety evaluation, Ind. Crops Prod. 181 (2022), 114816, https://doi.org/10.1016/j.indcrop.2022.114816.
[45] M. Huang, H. Zhuang, J. Zhao, J. Wang, W. Yan, J. Zhang, Differences in cellular damage induced by dielectric barrier discharge plasma between *Salmonella* Typhimurium and *Staphylococcus aureus*, Bioelectrochemistry 132 (2020), 107445, https://doi.org/10.1016/j.bioelechem.2019.107445.
[46] J. Sun, Z. Sun, D. Wang, F. Liu, D. Wang, Contribution of ultrasound in combination with chlorogenic acid against *Salmonella enteritidis* under biofilm and planktonic condition, Microb. Pathog. 165 (2022), 105489, https://doi.org/10.1016/j.micpath.2022.105489.
[47] Q. Shu, H. Lou, T. Wei, X. Zhang, Q. Chen, Synergistic antibacterial and antibiofilm effects of ultrasound and MEL-A against methicillin-resistant *Staphylococcus aureus*, Ultrason. Sonochem. 72 (2021), 105452, https://doi.org/10.1016/j.ultsonch.2020.105452.
[48] H. Yu, S. Chen, P. Cao, Synergistic bactericidal effects and mechanisms of low intensity ultrasound and antibiotics against bacteria: A review, Ultrason. Sonochem. 19 (3) (2012) 377–382, https://doi.org/10.1016/j.ultsonch.2011.11.010.
[49] R. Krishnamoorthy, M.A. Gassem, J. Athinarayanan, V.S. Periyasamy, S. Prasad, A. A. Alshatwi, Antifungal activity of nanoemulsion from *Cleome viscosa* essential oil against food-borne pathogenic *Candida albicans*, Saudi J. Biol. Sci. 28 (1) (2021) 286–293, https://doi.org/10.1016/j.sjbs.2020.10.001.
[50] G. Matafonova, V. Batoev, Review on low- and high-frequency sonolytic, sonophotolytic and sonophotochemical processes for inactivating pathogenic microorganisms in aqueous media, Water Res. 166 (2019), 115085, https://doi.org/10.1016/j.watres.2019.115085.
[51] M. Guo, L. Zhang, Q. He, S.A. Arabi, H. Zhao, W. Chen, X. Ye, D. Liu, Synergistic antibacterial effects of ultrasound and thyme essential oils nanoemulsion against *Escherichia coli* O157: H7, Ultrason. Sonochem. 66 (2020), 104988, https://doi.org/10.1016/j.ultsonch.2020.104988.
[52] J.-B. Park, J.-H. Kang, K.B. Song, Improving the microbial safety of fresh-cut endive with a combined treatment of cinnamon leaf oil emulsion containing cationic surfactants and ultrasound, J. Microbiol. Biotechnol. 28 (4) (2018) 503-509, https://doi.org/10.4014/jmb.1711.11018.
[53] Q. Ma, P.M. Davidson, Q. Zhong, Nanoemulsions of thymol and eugenol co-emulsified by lauric arginate and lecithin, Food Chem. 206 (2016) 167–173, https://doi.org/10.1016/j.foodchem.2016.03.065.
[54] K. Sharma, A. Babaei, K. Oberoi, K. Aayush, R. Sharma, S. Sharma, Essential oil nanoemulsion edible coating in food industry: a review, Food Bioproc. Tech. 15 (11) (2022) 2375–2395, https://doi.org/10.1007/s11947-022-02811-6.
[55] Q. Ru, Q. Hu, C. Dai, X. Zhang, Y. Wang, Formulation of *Laurus nobilis* essential oil nanoemulsion system and its application in fresh-cut muskmelons, Coatings 12 (2) (2022) 159, https://doi.org/10.3390/coatings12020159.
[56] W. Wu, H. Gao, H. Chen, X. Fang, Q. Han, Q. Zhong, Combined effects of aqueous chlorine dioxide and ultrasonic treatments on shelf-life and nutritional quality of bok choy (*Brassica chinensis*), LWT Food Sci. Technol. 101 (2019) 757–763, https://doi.org/10.1016/j.lwt.2018.11.073.
[57] Q. He, M. Guo, T.Z. Jin, S.A. Arabi, D. Liu, Ultrasound improves the decontamination effect of thyme essential oil nanoemulsions against *Escherichia coli* O157: H7 on cherry tomatoes, Int. J. Food Microbiol. 337 (2021), 108936, https://doi.org/10.1016/j.ijfoodmicro.2020.108936.